Density Functional Theory Model of Adsorption Deformation

Peter I. Ravikovitch and Alexander V. Neimark*

Center for Modeling and Characterization of Nanoporous Materials, TRI/Princeton, 601 Prospect Avenue, Princeton, New Jersey 08542

Received April 21, 2006. In Final Form: September 20, 2006

Molecules adsorbed in pores cause elastic deformations of the solid matrix leading to either contraction or swelling of the material. Although experimental manifestation of adsorption-induced deformation in clays, coals, carbons, silicas, and other materials has been known for a long time, a rigorous theoretical description of this phenomenon is lacking. We report the nonlocal density functional theory (NLDFT) calculations that reproduce almost quantitatively the adsorption and strain isotherms of Kr and Xe on zeolite X. This system exhibits characteristic contraction at low vapor pressures and swelling at high vapor pressures. We show that the experimentally observed changes in the adsorbent volume are proportional to the solvation (disjoining) pressure caused by the adsorption stress exerted on the pore walls. The proposed NLDFT model can be used for the interpretation of adsorption measurements in micro- and mesoporous materials and for the characterization of their mechanical properties.

Introduction

The phenomenon of adsorption-induced deformation is well documented in the literature.[1−12] Various explanations and macroscopic thermodynamic theories have been proposed for the mechanisms of dimensional changes of materials in the processes of adsorption and desorption.[1−3,5,10,13] In compliant materials such as gels, these deformations are quite pronounced.[14,15] In microporous materials such as carbons and zeolites, the reported magnitude of the adsorption-induced strain is usually on the order of $10^{-4}-10^{-3}$, which may seem to be a small value. However, elastic moduli may be on the order of gigapascals.[16] This implies large internal stresses on the order of megapascals. Such large stresses may play a crucial role in the stability of geological formations during the sequestration of carbon dioxide,[17,18] load-bearing composite systems, thin porous coatings, and membranes for electronic systems.[19] The development of novel low-dielectric-constant films[20,21] has triggered recent interest in revisiting the problem of adsorption-induced deformation. Low-*k* films are characterized by ellipsometric porosimetry, which measures vapor adsorption isotherms and associated changes in the film thickness (strain).[22] A method has been proposed for the determination of the Young's modulus of thin porous films from capillary condensation measurements using the Laplace equation.[20] However, many of the prospective low-*k* materials possess nanometer-size pores,[21,23−25] to which the macroscopic concepts of capillary contraction are not applicable. Moreover, experimental studies of the adsorption of gases and vapors in zeolites,[6,7] microporous carbons,[12] porous silicon,[19] and low-*k* films[20] demonstrate a characteristic common trend: at low vapor pressure, the system undergoes contraction followed by swelling at higher vapor pressure. Thus, strain as a function of vapor pressure (or adsorption) exhibits a nonmonotonic behavior that cannot be explained, even on a qualitative basis, by the macroscopic thermodynamics of capillarity, which employs the Laplace equation to assess the stress causing the contraction of the material.

Molecular simulations and density functional theory (DFT) provide a direct route to calculating the adsorption stress σ_s exerted on the solid by the molecules adsorbed in pores. The difference between the adsorption stress and external pressure, $f_s = \sigma_s - p_{ext}$, is called the solvation or disjoining pressure in the literature.[26] The complex nonmonotonic behavior of the solvation pressure as a function of pore size has been found for model fluids confined between parallel walls[26−31] as well as for clay interlayers.[32,33]

* Corresponding author. Present address: Department of Chemical and Biochemical Engineering, Rutgers, The State University of New Jersey, 98 Brett Road, Piscataway, New Jersey 08854-8058 E-mail: aneimark@rci.rutgers.edu.

(1) Bangham, D. H.; Fakhoury, N. *Nature (London)* **1928**, *122*, 681−682.
(2) Haines, R. S.; McIntosh, R. *J. Chem. Phys.* **1947**, *15*, 28−38.
(3) Yates, D. J. C. *Proc. R. Soc. London, Ser. A* **1954**, *224*, 526−544.
(4) Lakhanpal, M. L.; Flood, E. A. *Can. J. Chem.-Rev. Can. Chim.* **1957**, *35*, 887−899.
(5) Bering, B. P.; Krasilnikova, O. K.; Serpinskii, V. V. *Dokl. Akad. Nauk SSSR* **1976**, *231*, 373−376.
(6) Bering, B. P.; Krasilnikova, O. K.; Sarakhov, A. I.; Serpinskii, V. V.; Dubinin, M. M. *Bull. Acad. Sci. USSR Div. Chem. Sci.* **1977**, *26*, 2258−2261.
(7) Krasilnikova, O. K.; Bering, B. P.; Serpinskii, V. V.; Dubinin, M. M. *Bull. Acad. Sci. USSR Div. Chem. Sci.* **1977**, *26*, 1099−1101.
(8) Scherer, G. W. *J. Non-Cryst. Solids* **1986**, *87*, 199−225.
(9) Scherer, G. W. *J. Am. Ceram. Soc.* **1986**, *69*, 473−480.
(10) Jakubov, T. S.; Mainwaring, D. E. *Phys. Chem. Chem. Phys.* **2002**, *4*, 5678−5682.
(11) Yakovlev, V. Y.; Fomkin, A. A.; Tvardovskii, A. V.; Sinitsyn, V. A. *Russ. Chem. Bull.* **2005**, *54*, 1373−1377.
(12) Fomkin, A. A. *Adsorption* **2005**, *11*, 425−436.
(13) Ash, S. G.; Everett, D. H.; Radke, C. *J. Chem. Soc., Faraday Trans. 2* **1973**, *69*, 1256−1277.
(14) Reichenauer, G.; Scherer, G. W. *J. Non-Cryst. Solids* **2000**, *277*, 162−172.
(15) Herman, T.; Day, J.; Beamish, J. *Phys. Rev. B* **2006**, *73*, 094127.
(16) Colligan, M.; Forster, P. M.; Cheetham, A. K.; Lee, Y.; Vogt, T.; Hriljac, J. A. *J. Am. Chem. Soc.* **2004**, *126*, 12015−12022.
(17) White, C. M.; Smith, D. H.; Jones, K. L.; Goodman, A. L.; Jikich, S. A.; LaCount, R. B.; DuBose, S. B.; Ozdemir, E.; Morsi, B. I.; Schroeder, K. T. *Energy Fuels* **2005**, *19*, 659−724.
(18) Viete, D. R.; Ranjith, P. G. *Int. J. Coal Geol.* **2006**, *66*, 204−216.
(19) Dolino, G.; Bellet, D.; Faivre, C. *Phys. Rev. B* **1996**, *54*, 17919−17929.
(20) Mogilnikov, K. P.; Baklanov, M. R. *Electrochem. Solid State Lett.* **2002**, *5*, F29−F31.
(21) Boissiere, C.; Grosso, D.; Lepoutre, S.; Nicole, L.; Bruneau, A. B.; Sanchez, C. *Langmuir* **2005**, *21*, 12362−12371.
(22) Baklanov, M. R.; Mogilnikov, K. P.; Polovinkin, V. G.; Dultsev, F. N. *J. Vac. Sci. Technol., B* **2000**, *18*, 1385−1391.
(23) Padovani, A. M.; Rhodes, L.; Riester, L.; Lohman, G.; Tsuie, B.; Conner, J.; Allen, S. A. B.; Kohl, P. A. *Electrochem. Solid State Lett.* **2001**, *4*, F25−F28.
(24) Grill, A.; Patel, V.; Rodbell, K. P.; Huang, E.; Baklanov, M. R.; Mogilnikov, K. P.; Toney, M.; Kim, H. C. *J. Appl. Phys.* **2003**, *94*, 3427−3435.
(25) Lee, B. D.; Park, Y. H.; Hwang, Y. T.; Oh, W.; Yoon, J.; Ree, M. *Nat. Mater.* **2005**, *4*, 147−150.
(26) Balbuena, P. B.; Berry, D.; Gubbins, K. E. *J. Phys. Chem.* **1993**, *97*, 937−943.
(27) Lane, J. E.; Spurling, T. H. *Chem. Phys. Lett.* **1979**, *67*, 107−108.
(28) Snook, I. K.; Vanmegen, W. *J. Chem. Phys.* **1980**, *72*, 2907−2913.
(29) Evans, R.; Marconi, U. M. B. *J. Chem. Phys.* **1987**, *86*, 7138−7148.
(30) Evans, R.; Marconi, U. M. B.; Tarazona, P. *J. Chem. Phys.* **1986**, *84*, 2376−2399.

10.1021/la061092u CCC: $33.50
Published on Web 11/07/2006

However, few attempts have been made to relate the calculated solvation pressures to the material deformation measured in the course of adsorption, and all of them were based on the slit pore model.[34,35] Also, only a very limited number of molecular simulations addressed the flexibility of the porous network.[36]

In this work, we present a molecular-level approach for the correlation of adsorption and strain measurements and the calculation of the mechanical properties of nanoporous materials with spheroidal pores. We show that the adsorption-induced stress in the porous matrix is related to the solvation pressure calculated in the framework of the nonlocal density functional theory (NLDFT). The theoretical results are compared with the experimental strain isotherms of Kr and Xe in faujasite-type CaNaX zeolites.[6,7] These crystalline microporous materials, which possess a uniform 3D pore structure composed of ~12.3 Å cavities connected by ~7.4 Å windows, are suitable model adsorbents for studies of adsorption deformation. Moreover, their mechanical properties are of special interest because zeolites have been proposed as candidate materials for low-*k* layers.[37] The NLDFT model that we present below for spheroidal pores can be extended to pores of other shapes and to systems with polydisperse distributions of pore size.

Density Functional Theory of the Elastic Stress in Materials with Spheroidal Pores

Consider a porous body with a network of spheroidal pores, which is a crude representation of the pore structure in faujasite zeolites. The density of pores (i.e., the number of pores per unit volume) N_p is related to the body porosity ϕ:

$$N_p = \frac{3\phi}{4\pi R^3} \tag{1}$$

We make several assumptions about the elastic deformation of the porous body in the process of adsorption. First, we assume that the deformation is isotropic and is characterized by the volumetric strain $\epsilon = \Delta V/V_0$, where ΔV is the volume change compared to the initial volume V_0 of the body not being exposed to the adsorptive. Then, we adopt Hooke's law to relate the elastic stress σ and volumetric strain ϵ through the bulk modulus K

$$\sigma = K\epsilon \tag{2}$$

and express the elastic free energy as

$$F_e = V\int_0^\epsilon K\epsilon\, d\epsilon \tag{3}$$

For an isotropic solid, the bulk modulus K is related to Young's modulus E and the Poisson ratio ν as $K = E/3(1-2\nu)$. Note that equation 3 does not imply that the bulk modulus is constant, and thus it accounts for a possible nonlinear strain−stress relation.[38] In general, K depends on the porosity and pore structure morphology and may vary as adsorption progresses.

Second, we assume that the density of the solid framework itself is unchanged and the differential volume change of the sample $d(\Delta V) = V_0\, d\epsilon$ causes the respective alteration of the pore volume, $V_0\, d\epsilon = N_p V_0 d(4\pi R^3/3)$, and the pore radius, $dR = {}^1/_3 R\, d\epsilon/\phi$. The free energy of the adsorbed phase in deformed pores is uncoupled from the elastic free energy and can be calculated by using the standard NLDFT routine for the pore of given size R (see below). Thus, the free energy of the adsorbed phase equals

$$F_a = N_p V_0 F_p(N, V_p, T) \tag{4}$$

where $F_p(N, V_p, T)$ is the free energy of the adsorbed phase in a single pore of volume $V_p = 4\pi R^3/3$ that contains N molecules of adsorbate at temperature T.

Third, we assume that the total free energy is the sum of the elastic and adsorption free energies, and its variation at given chemical potential μ, external pressure p_{ext}, and temperature T is written as

$$d(F_a + F_e) = \mu N_p V_0\, dN - p_{ext} V_0\, d\epsilon \tag{5}$$

At a given chemical potential μ,

$$N_p V_0 d(F_p - \mu N) + KV_0\epsilon\, d\epsilon = -p_{ext} V_0\, d\epsilon \tag{6}$$

or invoking the definition of the grand thermodynamic potential of the adsorbed phase in the individual pore, $\Omega_p = F_p - \mu N$,

$$\frac{3\phi}{4\pi R^3} d\Omega_p + K\epsilon\, d\epsilon = -p_{ext}\, d\epsilon \tag{7}$$

The grand thermodynamic potential Ω_p is the function of the chemical potential μ, temperature T, and pore volume $\Omega_p = \Omega_p(\mu, V(R), T)$. The first term on the right-hand side of eq 7 can be expressed through the adsorption stress σ_s exerted by the adsorbed phase on the pore walls,

$$\sigma_s(R) = -\frac{1}{4\pi R^2}\left(\frac{\partial \Omega_p}{\partial R}\right)\Big|_{\mu,T} \tag{8}$$

Thus, accounting for $dR = {}^1/_3 R\, d\epsilon/\phi$, we arrive at the equation

$$\sigma = K\epsilon = -\frac{1}{4\pi R^2}\left(\frac{\partial \Omega_p}{\partial R}\right)\Big|_{\mu,T} - p_{ext} = \sigma_s - p_{ext} = f_s \tag{9}$$

which relates the volumetric strain ϵ to the solvation pressure f_s through the bulk modulus K.

It is worth noting that in the limit of large pores filled with liquid the solvation pressure f_s approaches the capillary pressure $p_{cap} = p_l - p_{ext}$, with p_l being the pressure in a condensed liquid. Respectively, the elastic stress equals the capillary pressure, which is related to the relative vapor pressure p/p_0 through the Kelvin equation $\sigma = p_{cap} = RT/V_l \ln p/p_0$. Although this capillary approximation is frequently used,[14,20,21] its applicability is limited to relatively large pores. Within the capillary approximation, the elastic stress is always negative, and its magnitude decreases as the vapor pressure increases, which implies shrinkage in the process of drying and swelling in the process of adsorption.

To calculate the adsorption stress (eq 8), one has to employ a certain dependence of the grand thermodynamic potential on the pore size. We apply the NLDFT model for spherical pores[39] to calculate the grand thermodynamic potential in a pore of size R. Within the NLFDT framework, the grand thermodynamic

(31) Schoen, M.; Diestler, D. J.; Cushman, J. H. *J. Chem. Phys.* **1994**, *100*, 7707−7717.
(32) Shroll, R. M.; Smith, D. E. *J. Chem. Phys.* **1999**, *111*, 9025−9033.
(33) Tambach, T. J.; Hensen, E. J. M.; Smit, B. *J. Phys. Chem. B* **2004**, *108*, 7586−7596.
(34) Samuel, J.; Brinker, C. J.; Frink, L. J. D.; van Swol, F. *Langmuir* **1998**, *14*, 2602−2605.
(35) Frink, L. J. D.; van Swol, F. *Langmuir* **1999**, *15*, 3296−3301.
(36) Shen, J.; Monson, P. A. *Mol. Phys.* **2002**, *100*, 2031−2039.
(37) Wang, Z. B.; Mitra, A. P.; Wang, H. T.; Huang, L. M.; Yan, Y. H. *Adv. Mater.* **2001**, *13*, 1463−1466.
(38) Wang, Z.; Lambros, J.; Lobo, R. F. *J. Mater. Sci.* **2002**, *37*, 2491−2499.
(39) Ravikovitch, P. I.; Neimark, A. V. *Langmuir* **2002**, *18*, 1550−1560.

Table 1. Parameters of the Intermolecular Potentials[a]

	Xe	Kr
ϵ_{ff}/k_B, K[b]	227.6	162.6
σ_{ff}, Å[b]	3.901	3.627
ϵ_{sf}/k_B, K[c]	128.2	109.6
σ_{sf}, Å[c]	3.586	3.450

[a] Framework oxygen number density $\rho_S = 0.177$ Å^{-2}. [b] From ref 47. [c] From ref 48.

potential $\Omega_p = \Omega_p(\mu, V(R), T)$ is found from the minimization of the grand thermodynamic potential functional $\Omega[\rho(r)]$ with respect to the fluid density distribution $\rho(r)$:[40]

$$\Omega[\rho(r)] = F_{id}[\rho(r)] + F_{ex}[\rho(r)] + \frac{1}{2}\int\int dr\, dr'\, \rho(r)\, \rho(r')\, u_{ff}(|r - r'|) - \int d\mathbf{r}\, \rho(r)[\mu - U_{ext}(R, r)] \quad (10)$$

Here $F_{id}[\rho]$ and $F_{ex}[\rho]$ are the ideal and excess components, respectively, of the Helmholtz free energy of the reference hard sphere (HS) fluid, $U_{ext}(R, r)$ is the fluid−solid intermolecular potential, which depends on the pore radius R, and $u_{ff}(|r - r'|)$ is the attractive part of the fluid−fluid intermolecular potential treated in a mean-field fashion using the WCA scheme.[41] For the free-energy functional of HS fluid $F_{ex}[\rho]$, we invoke Rosenfeld's fundamental measure theory (FMT),[42] which gives very good results in effectively zero-dimensional confinements such as spherical cavities.[43] Explicit expressions can be found elsewhere.[42,44,45]

We model faujasite pores as spherical cavities of radius R = 7.5 Å (measured to the center of the first layer of solid atoms). We apply the solid−fluid potential obtained by integration of the Lennard-Jones (LJ) potential over the spherical surface.[46] (See ref 39 for explicit equations.) Kr and Xe are modeled as LJ fluids with the energetic ϵ_{ff} and distance σ_{ff} parameters taken from ref 47. The parameters of the Kr−O and Xe−O interaction potential were calculated from the Lorentz−Berthelot mixing rules based on the reference Ar−O potential for high-silica zeolites as determined in ref 48 (Table 1). The only adjustable parameter in our calculations was the effective density of oxygen atoms, which was found to be $\rho_S = 0.177$ Å^{-2} to match the pore-filling step on the experimental isotherms (Figure 1a). It should be noted that this density is somewhat higher than the effective density of oxygen atoms describing Ar adsorption in NaY (ρ_S = 0.15 Å^{-2}),[49] which effectively accounts for the presence of cations in CaNaX.

Minimization of the functional (eq 10) was done following the standard DFT scheme (e.g., ref 44). Furthermore, the adsorption stress $\sigma_s(R)$ was determined by the differentiation of the grand thermodynamic potential Ω_p according to eq 8. The derivative in eq 8 has been calculated numerically using NLDFT calculations of Ω_p in pores of size R and $(R + \Delta R)$, where $\Delta R/R$ was on the order of 0.005−0.01. We have verified that the choice of ΔR does not affect the value of the calculated solvation pressure $f_s(R)$, which is compared with experimental data.

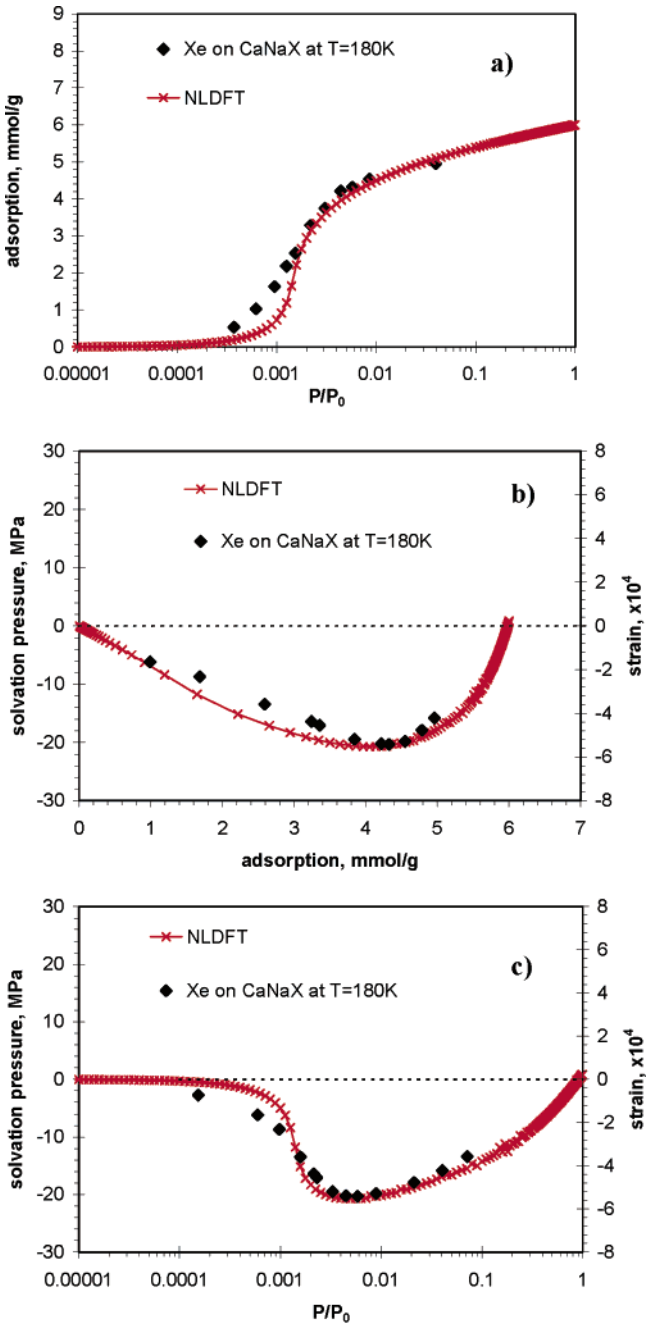

Figure 1. (a) Experimental (points)[7] and NLDFT calculated (lines) adsorption isotherms of Xe on zeolite CaNaX at 180 K. (b) Experimental strain (points, right vertical axis) and calculated solvation pressure (line, left axis) as a function of the amount adsorbed. (c) Same as in plot b but as a function of the bulk relative pressure P/P_0.

Results and Discussion

In Figure 1a, we compare the experimental and calculated adsorption isotherms of Xe on zeolite CaNaX at T = 180 K. The total loading of Xe at $P/P_0 = 1$ was estimated to be $n_{max} = 6$ mmol/g. Using the NLDFT density of confined Xe at $P/P_0 = 1$, we estimated the available pore volume of CaNaX as V_{pore} = 0.35 cm^3/g, which corresponds to the spherical cavity of R_{in} = 6 Å and agrees with the theoretical pore volume for faujasite

(40) Evans, R. In *Fundamentals of Inhomogeneous Fluids*; Henderson, D., Ed.; Marcel Dekker: New York, 1992; Chapter 5.
(41) Weeks, J. D.; Chandler, D.; Andersen, H. C. *J. Chem. Phys.* **1971**, *54*, 5237−5247.
(42) Rosenfeld, Y. *Phys. Rev. Lett.* **1989**, *63*, 980−983.
(43) Rosenfeld, Y.; Schmidt, M.; Lowen, H.; Tarazona, P. *Phys. Rev. E* **1997**, *55*, 4245−4263.
(44) Ravikovitch, P. I.; Vishnyakov, A.; Neimark, A. V. *Phys. Rev. E* **2001**, *64*, 011602.
(45) Yu, Y. X.; Wu, J. Z. *J. Chem. Phys.* **2002**, *117*, 10156−10164.
(46) Soto, J. L.; Myers, A. L. *Mol. Phys.* **1981**, *42*, 971−983.
(47) Vrabec, J.; Stoll, J.; Hasse, H. *J. Phys. Chem. B* **2001**, *105*, 12126−12133.
(48) Talu, O.; Myers, A. L. *Colloids Surf., A* **2001**, *187*, 83−93.
(49) Ravikovitch, P. I. Unpublished work.

Table 2. Structural Parameters of the CaNaX Zeolite as Determined from the NLDFT Model

	Xe	Kr
n_{max}, mmol/g[a]	6	7
V_{pore}, cm^3/g	0.35	0.31
bulk modulus, K, GPa	38	46

[a] Maximum adsorption.

zeolites (Table 2). The calculated Xe isotherm exhibits a somewhat sharper pore-filling step than the experimental one, which is due to simplifications of the spherical model of CaNaX cavities and the absence of cations in our model. Figure 1b and c show the experimentally measured volumetric strain during Xe adsorption[7] and the solvation pressure calculated from eq 9. The strain is initially zero and becomes negative (the sample contracts) as adsorption increases. The maximum measured negative strain is ca. -5.4×10^{-4}. After that, as adsorption progresses further, the sample expands. It can be seen that the calculated solvation pressure is proportional to the measured strain, and the agreement is almost quantitative in the full range of adsorption (vapor pressure). For Xe at 180 K, the external bulk pressure p_{ext} (eq 9) plays a minor role. The calculated maximal solvation pressure is $f_s = -20.7$ MPa, and we estimate the bulk modulus of CaNaX zeolites to be $K = 38$ GPa.

Qualitatively similar results have been obtained for Kr adsorption on the CaNaX zeolite at $T = 153$ K. From the comparison with the experimental adsorption isotherm,[6] we estimated the total loading of Kr at $P/P_0 = 1$ to be $n_{max} = 7$ mmol/g and the total pore volume to be $V_{pore} = 0.31$ cm^3/g, which is again in reasonable agreement with the pore structure of faujasites. However, there is a somewhat larger discrepancy in the shape of the experimental and calculated Kr isotherms. We attribute this to the deficiency of the simplified spheroidal representation of CaNaX cavities, which apparently becomes more important as the size of the guest molecule decreases (Kr vs Xe). Nevertheless, the calculated solvation pressure and the experimentally measured strain are in good agreement when plotted as a function of Kr loading (Figure 2b). Some discrepancy is apparent when these quantities are plotted as functions of the relative pressure (Figure 2c). These deviations can possibly be reduced by employing a nonlinear stress−strain relation. The maximum measured negative strain is -4×10^{-4}, and the corresponding solvation pressure is $f_s = -18.4$ MPa. Thus, the calculated bulk modulus of CaNaX obtained from Kr adsorption is $K = 46$ GPa, which is in reasonable agreement with the value obtained from Xe adsorption.

Given the simplified representation of the CaNaX structure and the fact that the only adjustable parameter in the calculations was the effective density of framework oxygens, we may conclude that the NLDFT provides an adequate, almost quantitative description of experimental adsorption and strain isotherms of Xe and Kr on zeolite CaNaX. The obtained bulk moduli of CaNaX can be compared with rather scarce data on the compressibility of faujasite and other zeolites. Colligan et al.[16] measured 38 GPa for pure silica NaY and 35 GPa for NaX by compression in a nonpenetrating silicone oil. The calculated modulus of NaY using an empirical interatomic potential for tetrahedral SiO_2 structures[50] was 59 GPa.[16] Thus, our values of 38 and 46 GPa fall between the reported experimental and calculated bulk moduli of faujasites. The original calculations of Bering and co-workers using the thermodynamic vacancy solution theory[5] gave the bulk modulus of the CaNaX zeolite as ca. 70 GPa, which seems to be too high.

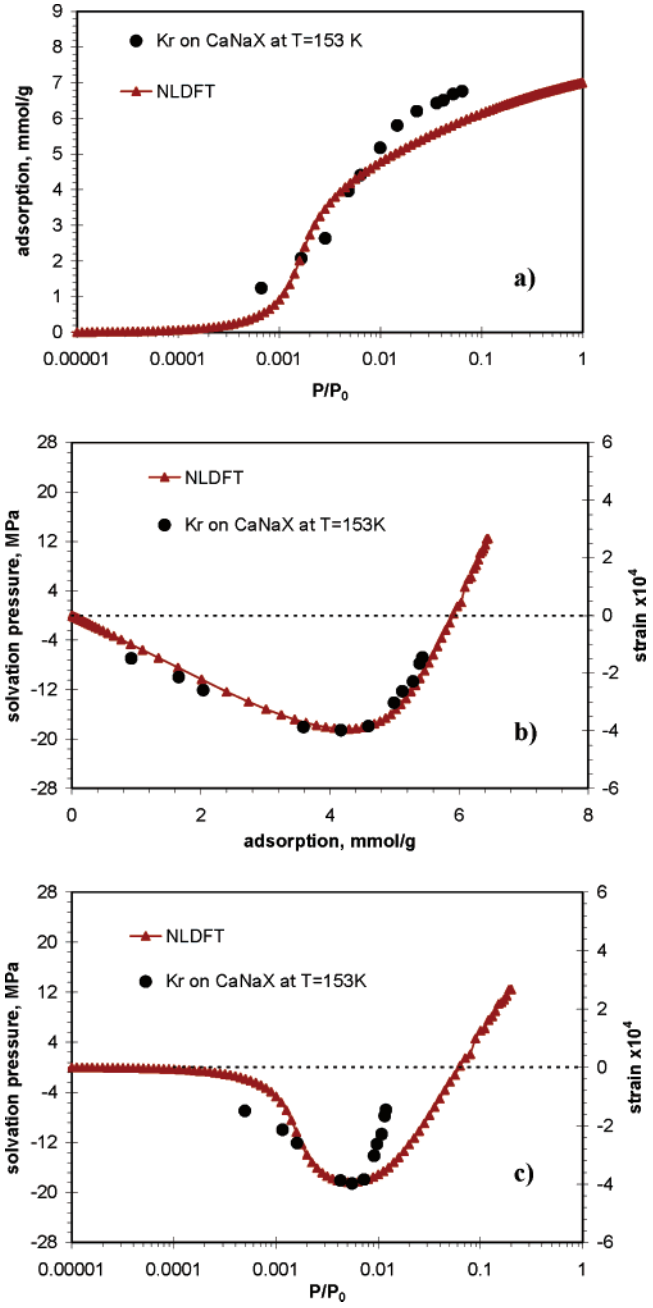

Figure 2. (a) Experimental (points)[6] and NLDFT calculated (lines) adsorption isotherms of Kr on zeolite CaNaX at 153 K. (b) Experimental strain (points, right vertical axis) and calculated solvation pressure (line, left axis) as a function of the amount adsorbed. (c) Same as in plot b but as a function of the bulk relative pressure P/P_0.

For comparison, the experimentally measured bulk modulus of the NaA zeolite is 22 GPa in glycerol [16,51] and 20−22 GPa in silicone oil.[52] The experimental value for α-quartz is 39 GPa,[53] and for α-cristobalite it was reported to be 11.5 GPa[54] and ∼16 GPa.[55] Astala et al.[56] calculated from electronic density functional theory the bulk moduli of α-quartz, α-cristobalite, sodalite (SOD),

(50) Sanders, M. J.; Leslie, M.; Catlow, C. R. A. *J. Chem. Soc., Chem. Commun.* **1984**, 1271−1273.
(51) Hazen, R. M.; Finger, L. W. *J. Appl. Phys.* **1984**, *56*, 1838−1840.
(52) Arletti, R.; Ferro, O.; Quartieri, S.; Sani, A.; Tabacchi, G.; Vezzalini, G. *Am. Mineral.* **2003**, *88*, 1416−1422.
(53) McSkimin, H. J.; Andreatch, P.; Thurston, R. N. *J. Appl. Phys.* **1965**, *36*, 1624−1632.
(54) Downs, R. T.; Palmer, D. C. *Am. Mineral.* **1994**, *79*, 9−14.
(55) Yeganeh-Haeri, A.; Weidner, D. J.; Parise, J. B. *Science* **1992**, *257*, 650−652.
(56) Astala, R.; Auerbach, S. M.; Monson, P. A. *J. Phys. Chem. B* **2004**, *108*, 9208−9215.

NaA (LTA), and silicalite (MFI) to be 38, 8, 18, 46, and 41 GPa, respectively. We estimated ~39 GPa for NaA from the simulations of Kim et al.,[57] who used the BKS potential.[58] However, micromechanical compressive response measurements of siliceous MFI zeolite single crystals gave an average Young's elastic modulus of only ca. ~4 GPa.[38] It is also important that the measured stress−strain curve for MFI zeolite was markedly nonlinear even for stresses <10 MPa[38] (e.g., those comparable with the predicted solvation pressures in zeolitic micropores). Given that we found only one reliable experimental piece of data for the bulk modulus of faujasites to compare with[16] and also quite diverse, method-dependent data for other zeolites, we may conclude that the bulk modulus of CaNaX calculated with the NLDFT model is in very reasonable agreement with the range of data reported for zeolitic materials. Finally, we note that some crystalline silicas (e.g., α-quartz and α-cristobalite) exhibit unusual mechanical properties such as negative Poisson's ratios.[55,59,60] In this case, one might expect significant anisotropy of the deformed framework that cannot be captured within our model.

In a companion paper,[61] we have calculated the solvation pressure isotherm of argon in mesoporous MCM-41 material with amorphous silica walls. The calculated solvation pressure exhibits nonmonotonic behavior, which is in qualitative agreement with the experimental strain isotherm measurements discussed above.[19−21]

Conclusions

The isotropic NLDFT model explains and describes almost quantitatively nonmonotonic adsorption-induced deformations typical for most zeolites and other microporous materials such as charcoal and activated carbon. This characteristic feature can be explained by a competition between the attraction of adsorbed molecules to the framework and the packing effects. Compression of the solid framework at low pressures is induced by dispersion attractive interactions with guest molecules. Adsorbed molecules serve as attractive "bridges" between the framework molecules, and the adsorption stress (eq 8) is negative so that the framework contracts. The condition of maximum contraction is determined from the condition of minimum adsorption stress:

$$\left(\frac{\partial \epsilon}{\partial \mu}\right)_{R,T} = -\frac{1}{4\pi R^2 K}\frac{\partial^2 \Omega_a}{\partial R \partial \mu} = -\frac{1}{4\pi R^2 K}\left(\frac{\partial N}{\partial R}\right)_{\mu,T} = 0 \tag{11}$$

The maximum contraction corresponds to the minimum of the adsorption stress that characterizes the "most comfortable" packing of adsorbed molecules in a cavity of a given size. The term "most comfortable" indicates the packing for which a virtual variation (both positive and negative because $(\partial N/\partial R)_{\mu,T} = 0$) of the pore size would lead to a decrease of adsorption at a given chemical potential and temperature. As the adsorption increases further, the repulsive interactions due to the densification of packing in the adsorbed phase come forward and the adsorption stress increases, and at a certain point, the solvation pressure may change sign and become positive (Figure 2b). Consequently, the material expands, and the volume of the saturated sample may exceed the volume of the evacuated (dry) sample. Certainly, a more detailed model, which would take into consideration the real morphology of the zeolites' framework, is desirable. However, it is likely that, with the exception for the absolute value of the bulk modulus, the results of more elaborate models will be qualitatively similar to the results obtained with the NLDFT model presented here.

Acknowledgment. This work was supported by the TRI/Princeton exploratory research program. A.V.N. gratefully acknowledges the support on the John Simon Guggenheim Memorial Foundation and fruitful discussion with G. Scherer. We thank M. Baklanov, T. Jakubov, and A. Tvardovski for useful correspondence.

LA061092U

(57) Kim, S. C.; Keskar, N. R.; McCormick, A. V.; Chelikowsky, J. R.; Davis, H. T. *J. Chem. Phys.* **1995**, *102*, 8656−8661.
(58) Van Beest, B. W. H.; Kramer, G. J.; Vansanten, R. A. *Phys. Rev. Lett.* **1990**, *64*, 1955−1958.
(59) Keskar, N. R.; Chelikowsky, J. R. *Nature (London)* **1992**, *358*, 222−224.
(60) Grima, J. N.; Jackson, R.; Alderson, A.; Evans, K. E. *Adv. Mater.* **2000**, *12*, 1912−1918.
(61) Ravikovitch P. I.; Neimark A. V. *Langmuir*, in press.